Neurocomputing 334 (2019) 265–274

Contents lists available at ScienceDirect

Neurocomputing

journal homepage: www.elsevier.com/locate/neucom

A classification method for multiple power quality disturbances using EWT based adaptive filtering and multiclass SVM

Karthik Thirumala [a,*], Sushmita Pal [b], Trapti Jain [b], Amod C. Umarikar [b]

[a] Department of Electrical and Electronics Engineering, NIT Tiruchirappalli, Trichy 620015, India
[b] Department of Electrical Engineering, IIT Indore, Indore 453552, India

ARTICLE INFO

Article history:
Received 5 April 2017
Revised 4 October 2018
Accepted 15 January 2019
Available online 23 January 2019

Communicated by Dr. A. Zobaa

Keywords:
Empirical wavelet transform (EWT)
Fast Fourier transform (FFT)
Power quality disturbances and Support vector machines (SVM)

ABSTRACT

This paper presents an automated recognition approach for the classification of power quality (PQ) disturbances based on adaptive filtering and a multiclass support vector machine (SVM). Empirical wavelet transform-based adaptive filtering technique is suitable for nonstationary signals and therefore has been adopted to extract features of PQ disturbances. It primarily estimates the actual frequencies present in the signal by means of the fast Fourier transform following a divide to conquer principle. Second, a set of adaptive filters is designed in the frequency domain to extract the mono-frequency components of a distorted signal. Then six efficient features reflecting the characteristics of disturbances are extracted from these components as well as the signal. Lastly, these features are fed as inputs to a multiclass SVM for classification of the most frequent PQ disturbances. The PQ disturbances considered in this work include eight single disturbances and seven two-combination disturbances. The simulation results elucidate the efficiency and robustness of the proposed approach against noise and different degrees of disorder. The performance of the one-against-one and one-against-all approach based SVM classifiers is compared to determine the best in terms of recognition accuracy and computation time. Further, the classifier is also verified on a few measured disturbance signals.

1. Introduction

Supply of reliable and quality power has become one of the key development objectives of the modern power sector. The growing dependency on the electronic control equipment, FACTS devices and renewable energy sources have enhanced the interest in power quality [1]. Also, the sensitivity of new-generation load is increasing because of which the consumers ranging from commercial buildings to industries are now demanding improvement in the quality of power delivered. All these made power quality monitoring a vital task besides load balancing and power factor correction [2,3]. A PQ disturbance usually comprises a deviation in voltage, current or fundamental frequency that interferes with the normal operation of the system or equipment [3]. In general, the power quality disturbances can be categorized into three major groups based on the waveform characteristics. They are amplitude variations, frequency variations and transient phenomenon. The voltage interruption, sag, swell and voltage fluctuations fall under the first category. Frequency variations cover harmonics, interharmonics, power frequency variations, voltage notching. Hence to identify the disturbances, the rate of occurrence and its sources, a large number of digital fault recorders and power quality meters have been deployed into the distribution system and industrial premises [4].

The visualization of recorded voltage/current waveform can reveal the class of disturbance manually, but it is not feasible to directly use the raw time-series data due to storage, management and interpretation issues. Additionally, the continuous monitoring is possible only if the detection system is automatic and fast. Therefore, the time-series waveform is sampled and processed to represent the waveform in terms of some finite set of features such as spectral content, amplitude, energy, the rate of rise, the rate of occurrence, duration of an event, etc. [5–8]. In fact, many signal processing techniques such as fast Fourier transform (FFT), wavelet transform (WT), S-transform (ST), Hilbert-Huang transform (HHT), tunable-Q wavelet transform (TQWT), variational mode decomposition (VMD) have been used to characterize the disturbances in time and frequency domains [6–15]. The features extracted from the aforementioned techniques are combined with some artificial intelligent tools such as fuzzy and rule-based expert systems, K nearest neighbor (K-NN), artificial neural network (ANN), and support vector machines (SVM) for recognition of disturbances [16–26]. The detection of only single disturbances is not a difficult task as they are distinct in nature and lot of work has been

* Corresponding author.
E-mail address: thirumala@nitt.edu (K. Thirumala).

https://doi.org/10.1016/j.neucom.2019.01.038
0925-2312/

done on this problem. In recent years, the PQ disturbances are often sequential or coexist in the distribution system causing new challenges for the system operator. These complex disturbances with two or more single events are difficult to recognize unless the fundamental frequency component is accurate or classifier is non-linear and robust [17,25–29].

Despite an extensive work carried out in this area, it is still a challenging problem due to the following reasons. The Fourier transform extracts the frequency information assuming the periodicity of a given signal, which results in spectral leakage. Also, the time information is lost. The discrete wavelet transform and wavelet packet transform provide multi-resolution analysis but are predefined and not self-adaptive. The selection of the mother wavelet and decomposition levels in advance is difficult and greatly influences the results. The ST developed based on the idea of the Gabor transform with Gaussian window and the WT has the ability to localize the variation in spectral characteristics. The higher computational complexity, window shape adjustment and spectral leakage problem of discrete Fourier domain are some issues that need to be addressed. The HHT represents the signal into the time-frequency domain using empirical mode decomposition (EMD) and Hilbert transform (HT). The EMD is completely adaptive based on time-series characteristics but has a major problem of mode mixing. This problem has been overcome or reduced by the VMD but at the cost of higher computational complexity. Considering the computational advantage, the practicality of the FFT, the IEC standard 61000-4-7 [30] recommends the use of the FFT for harmonic assessment of a 200 ms windowed signal. Therefore, efforts are being made for the development of new techniques based on FFT [31–34] to improve the accuracy by overcoming its limitations. The empirical wavelet transform (EWT) [35,36], which has gained lots of interest because of its adaptiveness, easy implementation and fastness, also uses the FFT for frequency estimation. Hence, the EWT based approach has been chosen for signal decomposition and feature extraction. The frequency estimation procedure of the EWT was modified in [37] using minimum frequency distance and minimum magnitude thresholds to make it suitable for analysis of voltage and current signals. However, the fixed thresholds, conceived to estimate the harmonics and interharmonics accurately, may give erroneous results in case of disturbance signals of 200 ms length. This can be overcome by divide to conquer principle based frequency estimation, inspired from [33], as explained in Section 2.2.

The design of classifier also plays an equally vital role in the detection and classification problems. The literature reveals that the rule-based decision tree classifiers are flexible to handle, but can detect only single disturbances accurately with thresholds according to the IEEE Std. 1159 [2] and IEC 61000-4-7 [30]. The expert systems fall under deterministic method and are normally slow in execution. Further, they lack self-learning capability and need an expert for rulemaking because of which they are not appropriate for PQ disturbances classification. The K-NN learning algorithm basically classifies new test data based on the closeness of the training data in feature space. The closeness is usually measured with Euclidean distance. The widely used ANNs are good at function approximation, data clustering and classification problems. They have salient features of self-learning, self-tuning and no need to know the input-output data relationship. However, the ANN structure is developed following a heuristic path, extensive experimentation and empirical risk minimization. Besides, the ANN suffers from multiple local minima, over-fitting and tuning of many network parameters. In the recent years, the support vector machine, which is a statistical learning approach, has gained greater interest due to the leading advantages of feature mapping and structural risk minimization principle. The mapping of non-linear separable data to a higher dimensional feature space for classification is another significance of the SVM. Also, the construction of the SVM involves the analysis and then experiments to tune only a few parameters as compared to the ANNs.

This paper utilizes the potentials of the EWT-based adaptive filtering technique and multiclass SVM for accurate classification of the most frequent fifteen disturbances with less computation time. The literature survey reveals that most of the SVM-based classification approaches developed for classification of combined disturbances are limited to at most eleven disturbances or use at least five features. Therefore, aims for classification of fifteen disturbances (eight single and seven combined) with only six features. The proposed approach can be summarized in four stages: (i) frequency estimation based on divide to conquer principle; (ii) adaptive signal decomposition; (iii) features extraction from the mono-frequency components and finally, (iv) employing a multiclass SVM for the classification of PQ disturbances. The first and second stages are explained in Section 2. The unique features extracted from the signal and filtered components are listed in Section 3.1. Thereafter, the extracted features are fed as inputs to the multiclass SVM for classification of fifteen PQ disturbances as explained in Section 3.2.

2. Methodology

2.1. Empirical wavelet transform

The empirical wavelet transform (EWT) [35] decomposes the time series signal into some distinct components based on the frequency information. The EWT method is easy to implement, customizable and appropriate to analyze nonstationary and time-varying signals. The steps to extract the individual components of the signal $x(n)$ are as follows

i) First, apply the FFT for the windowed signal to estimate the dominant frequencies present in the signal $f = \{f_i\}_{i=1,2,\ldots N}$.
ii) Identify the boundaries $\Omega = \{\Omega_i\}_{i=0,1,\ldots N}$, that separate the two consecutive frequency components and segment the complete Fourier spectrum. The first boundary Ω_0 is assumed to be zero and the rest $\Omega_i \forall i \in [1, N-1]$ are the local minima between two frequencies f_i, f_{i+1} [36] as shown in Fig. 1(a).
iii) Build N empirical wavelets, shown in Fig. 1(b), in the frequency domain corresponding to one low pass and $N-1$ bandpass filters using

$$\phi_1(\omega) = \begin{cases} 1 & if|\omega| \le (1-\gamma)\Omega_1 \\ \cos\left(\frac{\pi}{2}\beta(\gamma,\omega,\Omega_1)\right) & if(1-\gamma)\Omega_1 \le |\omega| \le (1+\gamma)\Omega_1 \\ 0 & otherwise \end{cases} \quad (1)$$

$$\psi_i(\omega) = \begin{cases} 1 & if\ (1+\gamma)\Omega_i \le |\omega| \le (1-\gamma)\Omega_{i+1} \\ cos\left(\frac{\pi}{2}\beta(\gamma,\omega,\Omega_{i+1})\right) & \text{if } (1-\gamma)\Omega_{i+1} \le |\omega| \le (1+\gamma)\Omega_{i+1} \\ sin\left(\frac{\pi}{2}\beta(\gamma,\omega,\Omega_i)\right) & \text{if } (1-\gamma)\Omega_i \le |\omega| \le (1+\gamma)\Omega_i \\ 0 & otherwise \end{cases} \quad (2)$$

where, $\beta(\gamma,\omega,\Omega_i) = \beta(1/2\gamma\Omega_i(|\omega| - (1-\gamma)\Omega_i))$ is an arbitrary function fulfilling the properties given in [35]. The parameter γ ensures very minimal overlap of the two consecutive transition areas, whose selection is based on the boundaries computed.
iv) Finally, the approximation and detail coefficients are obtained from the inverse fast Fourier transform of the filtered spectrum.

$$W_x(1,n) = IFFT(X(\omega)\phi_1(\omega)) \quad (3)$$

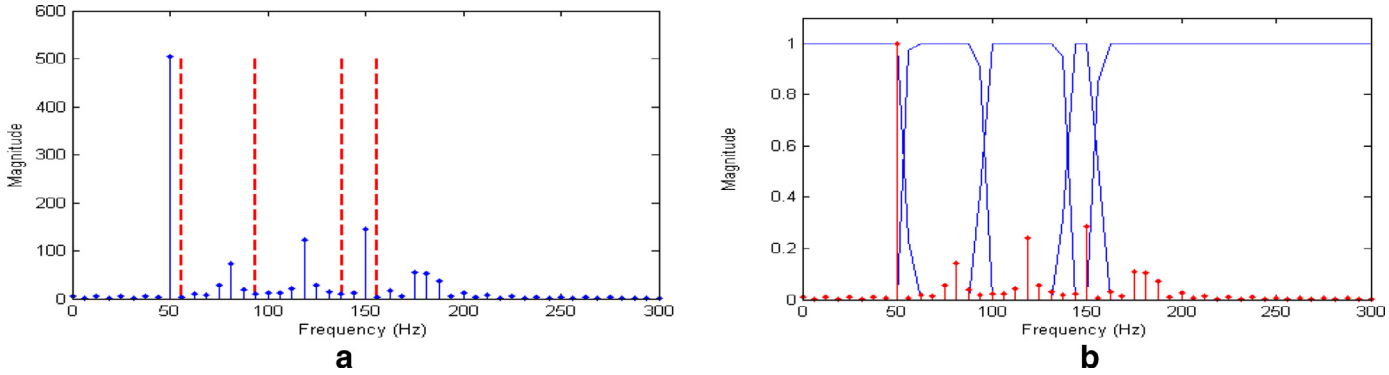

Fig. 1. (a) Segmented Fourier Spectrum. (b) Spectrum with the designed wavelet filters.

$$W_x(i,n) = IFFT(X(\omega)\psi_i(\omega)) \tag{4}$$

The segmentation of the Fourier spectrum is the most important step, which affects the performance of the EWT. Considering the advantages of the EWT, the frequency estimation step is modified in [37] to analyze the voltage and current signals. That approach uses minimum magnitude (dM) and minimum frequency distance threshold (dF) to avoid estimation of false frequencies. However, the thresholds chose assuming that the signals contain only harmonics and interharmonics may not give accurate results while analyzing other PQ disturbances. Therefore, the frequency estimation stage is further modified to make it suitable for analysis of various PQ disturbances.

2.2. Adaptive filtering technique

The EWT based adaptive filtering technique, shown in Fig. 2, aims at the perfect decomposition of the voltage/current signal yielding mono-frequency components. It has been observed that the disturbances like voltage sag, swell and interruption result in spectral leakage of the fundamental frequency component. The voltage fluctuation signals cause interharmonics near the fundamental frequency and the transient contains high frequencies. Therefore, the Fourier spectrum of a signal containing harmonics, interharmonics as well as amplitude variation looks composite. However, it can be inferred that the distance between two successive harmonics or two successive interharmonics is relatively more when compared to the distance between an interharmonic and harmonic. Considering these observations, divide to conquer principle based frequency estimation is opted for better segmentation of the Fourier spectrum. First, only dominant frequencies $\Lambda^1 = \{f_i\}_{i=1,2,\ldots M1}$ including the fundamental and harmonics are estimated using $dM = 2\%$ of the fundamental magnitude and $dF = 45$ Hz. Now design the empirical wavelets $\psi_i(\omega)$ given in (2) with these set of frequencies as center frequencies, $\Omega_i = f_i - 5$, $\Omega_{i+1} = f_i + 5$ Hz and $\gamma = 0.01$. The bandwidth of these bandpass filters can be given by $BW_i = 10 + 2\gamma f_i$ Hz. Then the harmonic spectrum $X_1(\omega)$ can be obtained using

$$X_1(\omega) = \left(\sum_{i \in \Lambda^1} X(\omega)\psi_i(\omega) \right) \tag{5}$$

The subtraction of harmonic spectrum $X_1(\omega)$ from the original spectrum $X(\omega)$ gives a residual spectrum $X_2(\omega)$, which contains only interharmonics. Then estimate the interharmonics $\Lambda^2 = \{f_i\}_{i=1,2,\ldots M2}$ by setting $dM = 2\%$ of the fundamental and $dF = 5$ Hz. Concatenate these two set of frequencies and arrange in ascending order to obtain the complete set of frequencies $\Lambda^3 = \{f_i\}_{i=1,2,\ldots M1+M2}$. For an extreme non-stationary signal, the information related to the fundamental component and dominant harmonics will still remain in the residual spectrum $X_2(\omega)$ due to spectral leakage. Therefore, in the cumulative set Λ^3, a grouping of directly adjacent components (±5 Hz) is performed to ensure that

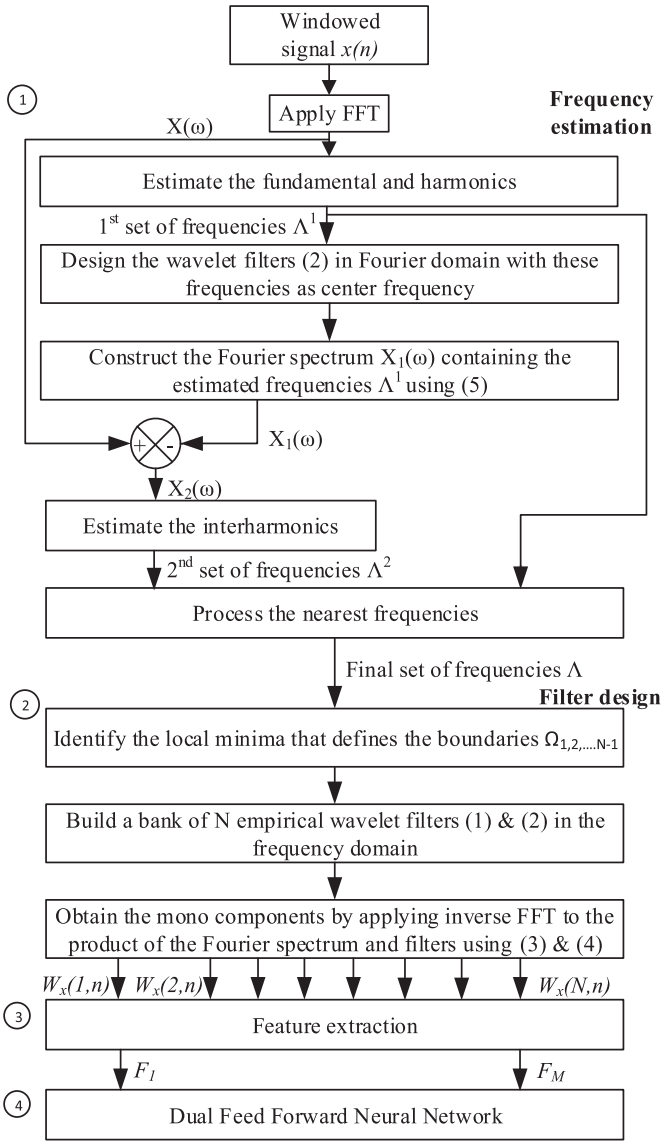

Fig. 2. Adaptive filtering technique for decomposition of input signal.

Table 1
Mathematical models of power quality disturbances.

Class label	PQD event	Equation	Parameters
C1	Normal	$x(t) = \sin(2\pi f_f t - \phi_f)$	$49.5 \le f_f \le 50.5,\ 0 \le \phi_f \le 180$
C2	Interruption	$x(t) = [1 - \alpha(u(t-t_1) - u(t-t_2))]\sin(2\pi f_f t - \phi_f)$	$0.9 \le \alpha \le 1, T \le t_2 - t_1 \le 9T$
C3	Sag	$x(t) = [1 - \alpha(u(t-t_1) - u(t-t_2))]\sin(2\pi f_f t - \phi_f)$	$0.1 \le \alpha \le 0.9, T \le t_2 - t_1 \le 9T$
C4	Swell	$x(t) = [1 + \alpha(u(t-t_1) - u(t-t_2))]\sin(2\pi f_f t - \phi_f)$	$0.1 \le \alpha \le 0.8, T \le t_2 - t_1 \le 9T$
C5	Harmonics	$x(t) = \sin(2\pi f_f t - \phi_f) + \sum a_i \sin(2\pi f_i t - \phi_i)$	$0.03 \le a_i \le 0.25$
C6	Flicker	$x(t) = [1 + \alpha \sin(2\pi \beta t)]\sin(2\pi f_f t - \phi_f)$	$0.1 \le \alpha \le 0.2,\ 5 \le \beta \le 25$
C7	Oscillatory Transient	$x(t) = \sin(2\pi f_f t - \phi_f) + \alpha_t \exp(-(t-t_1)/\tau)(u(t-t_1) - u(t-t_2))\sin(2\pi f_t t)$	$0.1 \le \alpha_t \le 0.8, 0.5T \le t_2 - t_1 \le 3T$ $300 \le f_t \le 3500, 8ms \le \tau \le 40ms$
C8	Notch	$x(t) = \sin(2\pi f_f t - \phi_f) -$ $\alpha sign(\sin(2\pi f_f t - \phi_f)) \times \{\sum_{n=0}^{9} u(t - (t_1 + 0.02n)) - u(t - (t_2 + 0.02n))\}$	$0.1 \le \alpha \le 0.4, 0 \le t_1, t_2 \le 5T$ $0.01T \le t_2 - t_1 \le 0.05T$
C9	Spike	$x(t) = \sin(2\pi f_f t - \phi_f) +$ $\alpha sign(\sin(2\pi f_f t - \phi_f)) \times \{\sum_{n=0}^{9} u(t - (t_1 + 0.02n)) - u(t - (t_2 + 0.02n))\}$	$0.1 \le \alpha \le 0.4, 0 \le t_1, t_2 \le 5T$ $0.01T \le t_2 - t_1 \le 0.05T$
C10	Sag + Harmonics	$x(t) = ([1 - \alpha \times (u(t-t_1) - u(t-t_2))]\sin(2\pi f_f t - \phi_f)) + \sum a_i \sin(2\pi f_i t - \phi_i)$	$0.1 \le \alpha \le 0.9, T \le t_2 - t_1 \le 9T$ $0.03 \le a_i \le 0.25$
C11	Swell + Harmonics	$x(t) = ([1 + \alpha \times (u(t-t_1) - u(t-t_2))]\sin(2\pi f_f t - \phi_f)) + \sum a_i \sin(2\pi f_i t - \phi_i)$	$0.1 \le \alpha \le 0.8, T \le t_2 - t_1 \le 9T$ $0.03 \le a_i \le 0.25$
C12	Sag + Transient	$x(t) = [1 - \alpha(u(t-t_1) - u(t-t_2))]\sin(2\pi f_f t - \phi_f) +$ $\alpha_t \exp(-(t-t_3)/\tau)(u(t-t_3) - u(t-t_4))\sin(2\pi f_t t)$	$0.1 \le \alpha \le 0.9, T \le t_2 - t_1 \le 9T$ $0.1 \le \alpha_t \le 0.8, 0.5T \le t_4 - t_3 \le 3T$ $300 \le f_t \le 3500, 8ms \le \tau \le 40ms$
C13	Swell + Transient	$x(t) = [1 + \alpha(u(t-t_1) - u(t-t_2))]\sin(2\pi f_f t - \phi_f) +$ $\alpha_t \exp(-(t-t_3)/\tau)(u(t-t_3) - u(t-t_4))\sin(2\pi f_t t)$	$0.1 \le \alpha \le 0.8, T \le t_2 - t_1 \le 9T$ $0.1 \le \alpha_t \le 0.8, 0.5T \le t_4 - t_3 \le 3T$ $300 \le f_t \le 3500, 8ms \le \tau \le 40ms$
C14	Flicker + Harmonics	$x(t) = ([1 + \alpha \sin(2\pi \beta t)] \times \sin(2\pi f_f t - \phi_f)) + \sum a_i \sin(2\pi f_i t - \phi_i)$	$0.1 \le \alpha \le 0.2,\ 5 \le \beta \le 25$ $0.03 \le a_i \le 0.25$
C15	Flicker + Transient	$x(t) = ([1 + \alpha \sin(2\pi \beta t)] \times \sin(2\pi f_f t - \phi_f)) +$ $\alpha_t \exp(-(t-t_1)/\tau)(u(t-t_1) - u(t-t_2))\sin(2\pi f_t t)$	$0.1 \le \alpha \le 0.2,\ 5 \le \beta \le 25$ $0.1 \le \alpha_t \le 0.8, 0.5T \le t_2 - t_1 \le 3T$ $300 \le f_t \le 3500, 8ms \le \tau \le 40ms$
C16	Transient + Harmonics	$x(t) = \sin(2\pi f_f t - \phi_f) + \sum a_i \sin(2\pi f_i t - \phi_i) +$ $\alpha_t \exp(-(t-t_1)/\tau)(u(t-t_1) - u(t-t_2))\sin(2\pi f_t t)$	$0.03 \le a_i \le 0.25,$ $0.1 \le \alpha_t \le 0.8, 0.5T \le t_2 - t_1 \le 3T$ $300 \le f_t \le 3500, 8ms \le \tau \le 40ms$

the actual frequencies are only considered for filter design to extract the mono-frequency components. Thus, the post-processing frequencies $\Lambda = \{f_i\}_{i=1,2,...N}$, $(N \le M1 + M2)$, are the final set of dominant frequencies that actually exist in a signal. Therefore, all the frequency components which are at least 10 Hz apart can be estimated and decomposed by obtaining the boundaries as explained earlier. Then design the empirical wavelet filters according to the frequency information. The components decomposed are of mono-frequency and thereby extracted features are significant for characterization of disturbances.

3. Feature extraction and classifier

The feature extraction is one of the most important stages of intelligent systems for classification. After decomposition of the signal into wavelet coefficients, the next step is to reduce the dimension of the data that is provided to a classifier by extracting a minimal set of features. In this paper, to detect fifteen PQ disturbances, six features are extracted from the original signal and its components. The PQ disturbances considered in this paper are eight single disturbances with class labels C2 – C9 and seven two-combination disturbances, C10 – C16 as listed in Table 1.

A pre-requisite for feature extraction is the estimation of an instantaneous amplitude of all the frequency components. The Hilbert transform (HT) [38] computes the complex conjugate of a real-valued signal and thereby, the analytic signal for estimation of instantaneous parameters. The analytic signal of a mono-frequency component $W_x(i, n)$, is defined as

$$\begin{aligned} AW_x(i,n) &= W_x(i,n) + jW_x^H(i,n) \\ &= IA(i,n)e^{j\theta_i(n)}\ \forall n = 1,..S \text{ and } i = 1,..N \end{aligned} \tag{6}$$

where $IA(i, n)$ is the instantaneous amplitude of a ith frequency component $W_x(i, n)$, n is the sample number and S is the number of samples within a window.

3.1. Feature extraction

One of the aims of this paper is to identify the minimal set of distinctive features for classification of single and combined disturbances. The most commonly employed features include amplitude RMS, total harmonic distortion (THD), frequency of the components, energy, mean of a cycle, etc. The following six features have been selected to distinguish the disturbances occurring.

F1: The feature $F1$, represents an absolute peak-to-peak difference of the signal magnitude over a window of 200 ms. An observation of disturbances reveals that the maxima and absolute minima of the voltage sag, swell, interruption, fluctuation and harmonics signals are almost same. Thereby, the $F1$ results very small values approximately zero for all the above-mentioned disturbances whereas the transient disturbance would be having a decaying magnitude. Hence, this feature plays a key role in distinguishing the transient and spike from rest of the disturbances.

$$F1 = |x_{\max} - |x_{\min}|| \tag{7}$$

where, $x_{\max}$ and $x_{\min}$ are the maxima and minima of the signal, respectively.

F2: The fundamental magnitude is very important in the identification of voltage sag, voltage swell, and interruption. The RMS value, which is the generally used feature, cannot accurately signify if the disturbance happens within a cycle or having magnitude at boundary conditions. This is due to the fact that the RMS is a squared average value calculated over one cycle or a complete time window. Therefore, to overcome this, we have considered the instantaneous amplitude (IA) of the fundamental frequency component obtained from the HT. This feature clearly differentiates the disturbances like voltage sag, interruption and swell.

$$F2 = \sqrt{\frac{1}{S}\sum_{n=1}^{S} IA(i,n)^2}\ \forall f_i \approx 50Hz \tag{8}$$

where S is the number of samples of the windowed signal and f_i is the frequency of ith component.

F3: The next feature is contrary to the *F2*, as this considers the total instantaneous amplitude of the distortion, defined as

$$F3 = \sqrt{\frac{1}{S}\sum_{n=1}^{S} TIDA(n)^2} \tag{9}$$

where $TIDA(n) = \sum_{i=1}^{N} IA(i,n)\ \forall i\ and\ f_i \neq 50$ is the sum of the amplitude of all the frequency components except fundamental and N is the number of frequencies estimated. The F3 would be near zero for normal signal, voltage sag, swell, interruption and very high value for distorted signals.

F4: The most commonly used total harmonic distortion (***THD***) helps in separation of all the harmonic related signals from the other classes. The ***THD*** is computed over each fundamental cycle up to ten and its mean is chosen as the feature.

$$F4 = mean(\boldsymbol{THD}) \tag{10}$$

$$THD(m) = \frac{X_{Hrms}(m)}{X_{1rms}(m)} \tag{11}$$

where, $X_{1rms}(m)$ is the *mth* cycle RMS value of the fundamental frequency component x_1 and $X_{Hrms}(m)$ is the distortion RMS except fundamental component calculated as

$$X_{1rms}(m) = \sqrt{\frac{1}{S}\sum_{n=(m-1)S+1}^{mS} x_1(n)^2}\ \text{and}\ X_{Hrms}(m) = \sqrt{\frac{1}{S}\sum_{n=(m-1)S+1}^{mS} x_h(n)^2} \tag{12}$$

F5: The ***THD***-per-cycle of steady-state harmonic disturbances remains almost same, whereas, for transient signals, the ***THD*** will be quite higher for at most two cycles and zero for the remaining cycles. As a result, the mean value of the ***THD*** will be dropped to very low value for the transient signal. Therefore, the maximum of ten ***THD*** values is selected as the fifth feature, which can differentiate the transient signals from the notch, spike and harmonics.

$$F5 = max(\boldsymbol{THD}) \tag{13}$$

F6: All the disturbances other than fundamental amplitude deviations, contains harmonic or interharmonics along with the fundamental frequency and it is a little bit complex to distinguish among them (C5 – C16) just by *THD*. A keen observation of characteristics of these disturbances reveals that the number of frequencies, their frequency range and intensities vary. For instance, transient frequencies and their magnitudes are relatively higher than the remaining and the voltage fluctuation has only two to three low-frequency components. Therefore, a new feature has been proposed to measure the distortion content excluding the fundamental in terms of instantaneous frequency of the components weighted by their amplitudes.

$$F6 = \max_{n}(TIDF) \tag{14}$$

where *TIDF* is the total instantaneous distortion factor calculated at each sample n, using the formula given by

$$TIDF(n) = \frac{1}{N}\sum_{i=1}^{N} IF(i,n)IA(i,n)\ \forall i\ and\ f_i \neq 50 \tag{15}$$

3.2. Multiclass SVM classifier

Support vector machine (SVM) developed by Cores and Vapnik, is a supervised learning machine, framed on statistical learning theory or Vapnik-Chervonenkis (VC) theory [39]. The SVM may be viewed as a binary classifier. It abstracts a decision boundary from the data and uses it to classify patterns belonging to the two alike classes. The margin $1/\|w\|$, which is a distance between optimal separating hyperplane and the instances on either side of it, is an important notation in the SVM. The vectors that lie on these margins are called support vectors. In a linear separable case, the solution is represented as a linear combination of only support vectors ignoring the other data. Therefore, in general, the complexity of the SVM model is unaffected by the number of features selected. The essence of the SVM lies in the projection of linearly non-separable input data to a high-dimensional feature space and finding an optimal hyperplane in the feature space with maximum possible margin. For a training set labelled as $\{X_i, y_i\}$, $i = 1, 2, \ldots l$ and l is the number of training samples, the problem of finding optimal hyperplane (16) over bias, b and weight vector w.

$$\min \frac{1}{2}\|w\|^2 + C\sum_{i=1}^{l}\xi_i \tag{16}$$

subject to $y_i(w^T x_i + b) \geq 1 - \xi_i$ and $\xi_i \geq 0$

where x is the input feature vector with class label $y \in \{-1, 1\}$. The first part of the problem (16) aims to maximize the margin between the two classes. The second term aims to reduce the training errors by penalizing the solutions of a large slack variable ξ_i with the cost of penalty, C. Larger C value makes constraints hard to ignore and hence, minimize the margin. This constrained quadratic programming problem can be solved in a simpler way using the Lagrangian multiplier method and formulating its dual problem with kernel trick as

$$max \sum_i \lambda_i - \frac{1}{2}\sum_i\sum_j \lambda_i\lambda_j y_i y_j K\left(X_i, X_j\right) \tag{17}$$

such that $\sum_i \lambda_i y_i = 0$ and $0 \leq \lambda_i \leq C, i = 1, \ldots, l$ and $\xi_j \geq 0$

where, λ_i is a Lagrangian multiplier. This dual problem with linear equality constraints can be solved with a simple sequential minimal optimization algorithm. The optimization problem of SVM reaches a global minimum rather than ending in a local minimum, which may happen in ANN. The increase in the dimensionality of the data by nonlinear feature mapping helps in separation of classes possibly by a linear hyperplane. The mapping is achieved using kernel function $K(x_i, x_j)$ and the most commonly used kernels are

1. Linear Kernel: $K(x_i, x_j) = x_i^T x_j$
2. Polynomial: $K(x_i, x_j) = (\gamma x_i^T x_j + r)^d, \gamma > 0$
3. Gaussian Radial Basis function: $K(x_i, x_j) = exp(-\gamma |x_i^T - x_j|^2)$
4. Sigmoid: $K(x_i, x_j) = \tanh(\gamma x_i^T x_j + r)$

The solution of the SVM classifier for an unknown feature vector X (testing) is

$$f(X) = sign\left(\sum_i^l \lambda_i y_i K(X_i, X) + b\right),\ f(X) \rightarrow \{-1, 1\} \tag{18}$$

SVM, originally developed for binary classification are successfully employed for multiclass classification problem by adopting a group of binary SVMs. The most commonly used ways for multiclass classification are one-against-all (OAA), one-against-one (OAO) and a directed acyclic graph SVM (DAGSVM) [40]. The OAO method performs pairwise classification by constructing $k(k-1)/2$ binary models for a k-class problem. In this method, each model is

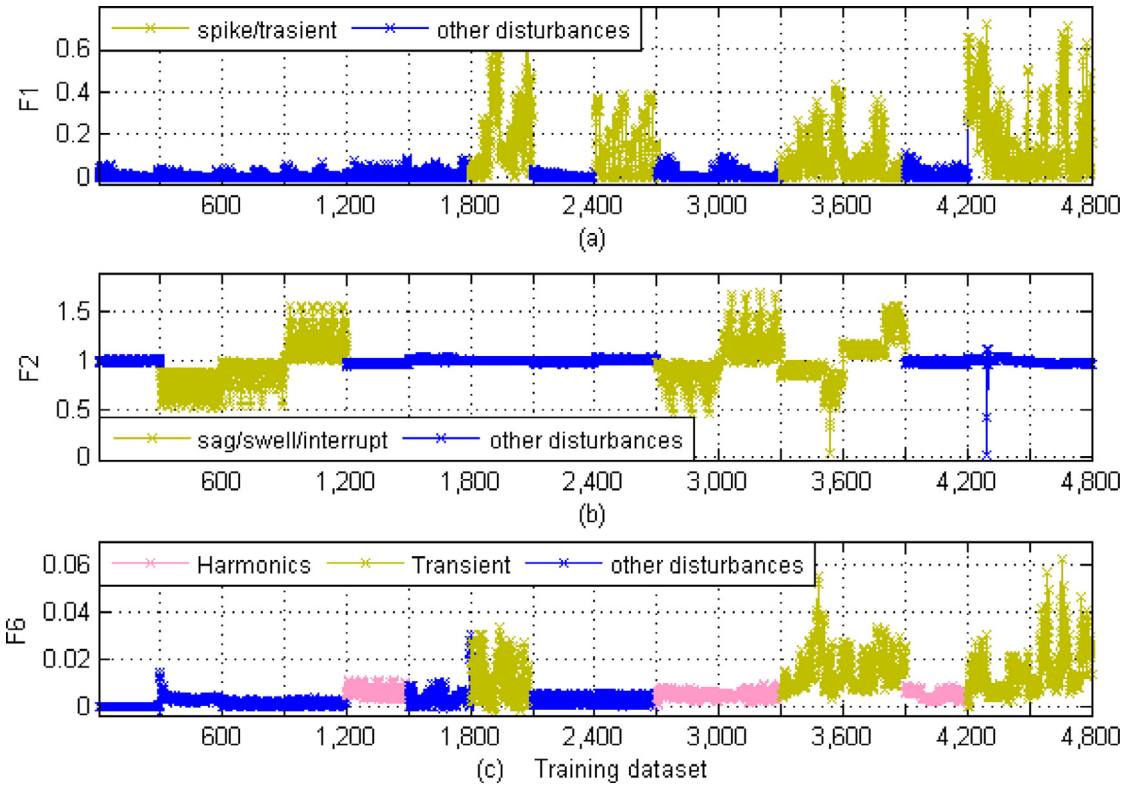

Fig. 3. Estimated feature values for the training data.

trained with the data of two unlike classes and thereby transform the k-class classification problem into $k(k-1)/2$ different tasks. Then, the prediction of the class for the test data is based on the maximum voting [40]. The other method, OAA solves the k-class problem by solving k number of two class classification tasks and therefore requires just k binary models, each dedicated for detection of a particular class. In this method, each binary SVM model is trained with complete data with the positive label only for current class and negative label for all other classes. Both these methods are considered suitable for multiclass classification problems [40]. Hence, the OAO and OAA methods based SVMs are opted for classification of PQ disturbances and the performance is compared in the next section. It is important to note that these classifiers are implemented in MATLAB with the help of LIBSVM toolbox [41].

4. Results and discussion

4.1. Evaluation studies on simulated disturbances

The multiclass SVM classifier needs to be trained with a large amount of data containing different degrees of irregularities and variations. Since it is very difficult to acquire a huge amount of real disturbance signals from the system, the classifier is trained with simulated data generated using the standard mathematical models [2,8,9] reported in Table 1. To evaluate the performance of the proposed approach for classification of fifteen disturbances and a normal signal, a total of 6400 signals with 400 signals of each class are generated by varying all the parameters. The signal parameters such as event duration, frequencies, amplitudes and their phase angles are wide-ranged according to the standards and literature [2,8,9,30]. The fundamental frequency of the signals is 50 Hz and randomly varied in a range of ±0.5 Hz. In addition, to verify the robustness of the proposed approach towards the noise, the signals are contaminated with a white Gaussian noise of different SNRs from 25 dB to 55 dB. All the signals are of 200 ms duration in accordance with the IEC standard 61000-4-7 [30] and sampled at 10 kHz resulting in 2000 samples per window. From the literature, it has been observed that the SVM requires large data for training as compared to the ANN. Considering this, the multiclass SVM classifier is trained with 75% of the total patterns and then tested on the remaining 25% data. A dataset of 20% of the training data is used for tuning the regularization parameters. The training and testing data is selected randomly. The optimal parameters and kernel functions are identified using an extensive grid search process. To evaluate the generalized performance, this paper also employs 10-fold cross validation for the proposed classifier. Further, the proposed approach has also been tested on five measured signals acquired from different sources. The experiments are carried out in MATLAB tool hosted on a PC with an Intel Core i5 3.1 GHz processor and 4 GB RAM.

Initially, the feature vectors are extracted for the complete 4800 training data patterns and 1600 test data patterns. Fig. 3 shows the plot of feature values estimated for the complete training data. It can be observed from Fig. 3(a) that the value of feature *F1*, is relatively higher for the disturbances (C7, C9, C12, C13, C15 and C16) containing either oscillatory transient or spike as expected. It is evident from Fig. 3(b) that the feature *F2*, based on the instantaneous fundamental amplitude, is clearly discriminating all the fundamental magnitude related disturbances. Similarly, Fig. 3(c) reveals that *F6* is able to discriminate the frequency distortion disturbances. The disturbances containing transient has very high value than the interharmonic/harmonic disturbances. The other frequency-based disturbances such as notch, spike and voltage fluctuations have less distortion value as they contain low-frequency components with a magnitude of 2–8% of the fundamental magnitude.

The features extracted on the basis of the adaptive filtering are employed to two multiclass SVM classifiers adopting one-against-one (OAO) and one-against-all (OAA) methods, respectively. The performance of both the classifiers with same kernels is evaluated in terms of classification accuracy and computation time. As the signal decomposition and features are same for both the classifiers, the time taken for decomposition and feature extraction also

Table 2
Performance comparison of the multiclass SVMs with different kernels.

Kernels	OAO-SVM classifier						OAA-SVM Classifier					
	Accuracy (%)		*Training time (s)*		*Testing time (s)*		*Accuracy (%)*		*Training time (s)*		*Testing time (s)*	
	9 class	*16 class*	*9 class*	*16 class*	*9 class*	*16 class*	*9 class*	*16 class*	*9 class*	*16 class*	*9 class*	*16 class*
Linear C = 10	93.55	89.06	0.044	0.432	0.006	0.035	79.7	55.26	49.198	532.9	0.023	0.088
RBF C = 90, $\gamma = 0.1$	97.22	88.12	0.029	0.166	0.009	0.043	94.45	85.1	0.660	3.836	0.038	0.107
Polynomial C = 12, d = 2, $\gamma = 0.97$, $r = 0$	97.22	95.56	1.113	20.73	0.005	0.027	83.95	78.13	327.4	1917	0.025	0.437
Sigmoid C = 100, $r = 0$, $\gamma = 0.0001$	88.77	68.62	0.034	0.092	0.016	0.070	66.45	36.2	0.469	1.934	0.038	0.133

Table 3
Confusion matrix for 16 classes using OAO-SVM classifier with polynomial kernel.

Predicted class																	
Actual class	C1	C2	C3	C4	C5	C6	C7	C8	C9	C10	C11	C12	C13	C14	C15	C16	Detection rate (%)
C1	96					3		1									96
C2		100															100
C3	1	3	94					2									94
C4				97		2			1								97
C5					96	1		2			1						96
C6	3					97											97
C7							98		2								98
C8	1		1		2			96									96
C9	1						2		94		3						94
C10			2		4				1	92				1			92
C11											100						100
C12			4					2				94					94
C13				5					2		1		92				92
C14	1				3	1			1					94			94
C15					4	2							1		93		93
C16					2						2					96	96
Overall Accuracy (%)																	95.56

remains same. Hence, only the training and testing times are investigated for fair comparison. The training time and testing time reported here are just the time taken by the classifier for training and testing, respectively excluding the decomposition time and feature extraction time. Although the main aim of this work is to recognize sixteen classes, Table 2 also presents the results obtained for the detection of the first nine classes C1–C9 (trained and tested separately), for better illustration. Further, the performance of the two multiclass SVM classifiers is evaluated by employing four different kernels. The kernel parameters *d*, γ and regularization parameter *C* are tuned by experimentation to achieve maximum recognition accuracy and the optimal values are reported in Table 2. Irrespective of the kernels, the OAO–SVM is detecting all the nine classes with more accuracy and less computation time as compared to the OAA–SVM. Though the OAA–SVM employs only nine binary models for nine classes, each model is trained with the complete data. This increases the number of variables of the optimization problem, which demands more time for computation. Whereas the OAO method uses 36 binary SVM models but each is trained with only data of two unlike classes. The same is evident from the results obtained; the training time of the OAA–SVM is at least fifteen times that of the OAO–SVM. In some cases like with polynomial kernel, it is taking approximately 327 s. It can be established that the OAO–SVM with either RBF or polynomial kernel, which is having an overall accuracy of 97.22% is recommendable for classification of single disturbances and a normal signal.

An observation of the results of the sixteen classes (C1–C16) indicates that the overall accuracy of both the classifiers is reduced for all kernels as compared to that of the nine classes. This is due to the combined disturbances, as they have either mixed characteristics of both the disturbances or dominated by anyone disturbance. For instance, flicker + transient signal with low transient factor can be considered as the simple harmonics class as shown in Table 3 due to very less values of *F3, F4* and *F5*. Table 3 lists the recognition accuracy of OAO–SVM with the polynomial kernel for all 16 individual classes. The drop in the overall accuracy of both the classifiers for sixteen classes is significant. However, the OAA–SVM with 2nd order polynomial kernel is able to distinguish the combined disturbances as well, along with the single disturbances. As a result, the recognition accuracy for the combined disturbances such as sag + harmonic, swell + transient, flicker + transient is noticed to be 92–93%, which is the least of all individual class accuracies as reported in Table 3. Finally, it can be concluded that the second order polynomial is performing better than other kernels with an overall accuracy of 95.56%.

The conclusions made on the training and testing time of OAO and OAA–SVMs for classification of nine classes are valid for sixteen classes as well. The training time of the OAO classifier with the polynomial kernel is increased to 20 s, but it is still very less than that of the OAA–SVM. Besides, it is a known fact that the classifier will be trained offline and uses the finally trained model for testing online data. So the testing time is a major concern for real-time classification of PQ disturbances but not the training time. Hence, the total computation time includes only signal decomposition time, feature extraction and testing time. The average total computation time of 20 multiple runs is found to be around 128 ms, of which the testing time is at most 27 ms for 16 classes. The signal decomposition time depends on the number of frequencies, sampling rate and time window length. An increase in the time window length would not only increase the buffering and computation time but also the probability of PQ disturbances. The contrary will reduce the estimation time but affects the recognition accuracy as the method skips estimation of low-frequency interharmonics below 50 Hz and suffers from picket fencing effect. Since the signals are buffered in the blocks of 200 ms for further processing and detection, the total computation time should be below 200 ms. From the results, it evident that the proposed approach of adaptive filtering and OAO–SVM classifier with

Table 4
Classification results for twenty-one classes.

Kernels	21 classes					
	OAO-SVM classifier			OAA-SVM Classifier		
	Accuracy (%)	*Training time (s)*	*Testing time (s)*	*Accuracy (%)*	*Training time (s)*	*Testing time (s)*
Linear C = 10	78.33	3.332	0.065	25.19	1131.8	0.206
RBF C = 90, γ = 0.99	67.23	1.201	0.142	27.38	23.094	0.545
Polynomial C = 12, d = 2, γ = 0.97, r = 0	88.48	48.685	0.041	26.8	4434.4	1.773
Sigmoid C = 168, r = 0, γ = 0.0001	75.52	0.18	0.147	35.52	3.958	0.475

Table 5
Classification results of OAO-SVM using 10-fold cross validation.

	Mean Accuracy			Standard deviation		
	9 classes	*16 classes*	*21 classes*	*9 classes*	*16 classes*	*21 classes*
Linear C = 10	93.81	88.48	75.12	0.8	1.23	0.94
RBF C = 90, γ = 0.99	98.37	86.63	69.89	0.87	0.76	0.71
Polynomial C = 12, d = 2, γ = 0.97, r = 0	98.53	94.26	89.49	0.64	0.67	0.8
Sigmoid C = 168, r = 0, γ = 0.0001	90.79	70.21	71.33	0.68	0.76	0.68

polynomial kernel is successfully fulfilling this criterion. Hence, the online detection of PQ disturbances is achievable with an implementation of the proposed approach on a digital signal processor (DSP) or FPGA.

To further verify the ability of the adaptive filtering-based features for classification of additional disturbances, experiments are conducted by extending the classes to twenty-one with the inclusion of five new disturbances. They are interruption + transient, sag + flicker, swell + flicker, sag + harmonics + transient and swell + harmonics + transient. First, the features are extracted for these disturbances as well and then retrained the classifier with data of twenty-one classes. Table 4 reports the results achieved for both the classifiers using optimal kernels. The kernel parameters are slightly varied to the best for maximum accuracy. It is observed that the misclassification rate and computation time are increasing with an increase in the number of classes and the performance of the OAA–SVM is completely degraded. It is interesting to notice that the linear kernel is giving more accurate results than the RBF and sigmoid in case of 16 and 21 classes, and almost same for nine classes. This linear separation capability proves the potentiality of the features extracted. The overall prediction rate of the OAO–SVM with a second order polynomial is around 88%, which is considerable for twenty-one classes and also, the testing time is just twice the fundamental cycle.

According to the results, the one-against-one approach based multiclass SVM with second order polynomial kernel is outperforming all other kernels and OAA–SVM in terms of both accuracy and testing time. Since the *k*-fold cross validation is a very reliable method for the generalized performance evaluation, this paper employs 10-fold cross validation, in which the SVM is trained with randomly selected 9 subsets of the total data and validated on the remained subset. The classification results obtained for the 9, 16 and 21 classes individually using the 10-fold cross validation are given in Table 5. From the 10-fold cross validation results, it can be noticed that the standard deviation is in the range of 0.64–0.94. The mean accuracies are slightly varied as compared to without cross-validation; however, the OAO–SVM with polynomial kernel is still a good predictor.

4.2. Measured signals

In this paper, five measured PQ disturbance signals have been used to demonstrate the ability of the proposed approach. They are two harmonic signals, voltage sag, normal voltage signal and a transient signal. The measured input signals are first normalized and then processed for detection of the disturbances. The sampling rate and features extracted for the measured signals are listed in Table 6. A harmonic current signal, shown in Fig. 4(a) is acquired in the laboratory from a (CFL) lamp load. The feature *F1* value clearly indicates that the signal is stationary, which is evident from Fig. 4(a). The values of *F4* and *F5* are almost same, which also confirms that the harmonic distortion is same throughout the signal. Therefore, the signal is correctly recognized by the classifier as C5 class. Similarly, the classifier is tested on a voltage harmonic signal acquired from the distribution system of an academic institution [42]. The observations made above are valid for this signal as well. It is bit difficult to acquire a voltage sag/swell signal, hence a recorded 60 Hz waveform, provided by the IEEE 1159.2 [43] is considered for validation. The Fig. 4(b) shows a phase-a voltage sag signal (wave 7) sampled at 15.36 kHz [43], which has sag for around two fundamental cycles. The *F2* = 0.831 undoubtedly indicates the dip in the fundamental voltage. Though the maximum THD, *F5* is as high as 0.316, the mean value is just 0.06. The THD is highest in the fifth cycle, where the sag initiates with slight distortion as seen in Fig. 4(b) and it is high due to the ratio relative to the lower fundamental amplitude (≈0.18). Finally, the transient current signal, shown in Fig. 4(c) is considered for validating the performance of the proposed approach. Switching on a PC while a laptop and a mobile are already charging has generated a switching transient, shown in Fig. 4(c). The transient signal is acquired at a rate of 12.8 kHz, using a current probe and OROS 34 data acquisition card. It can be observed that the *F6* = 0.038, *F1* = 1.605, *F3* = 1.876 and *F5* = 0.812, these features reflect the presence of the transient in one cycle and *F4* = 0.635 indicates that the harmonics are present in the signal consistently. Finally, the results evidence that the proposed approach is able to recognize the real disturbances.

The performance comparison of the proposed method with the other reported methods in terms of feature dimension, number of classes and classification accuracy is shown in Table 7. It can be observed that some methods have better accuracy but they detect lesser number of disturbances [8,14,15,44,46] or utilize more features as in [15,44,45]. The method proposed in [45] has better classification accuracy however, the computation time is almost four times of the proposed method. An increase in features may increase the classification accuracy but at the same time, it also increases the computational burden. Minimal set of features would reduce the memory requirement for data storage and also the computational burden. Consequently, a low-cost microcontroller or DSP would be sufficient for development of a standalone low-cost

Table 6
Classification results of measured disturbance signals.

Signals	Sampling rate	F1	F2	F3	F4	F5	F6	Class detected
Current harmonic (Fig. 4(a))	12.8 kHz	0.009	0.938	0.470	0.229	0.231	0.005	C5
Voltage harmonic [42]	6.4 kHz	0.004	0.989	0.383	0.201	0.204	0.005	C5
Voltage sag [43] (Fig. 4(b))	15.36 kHz	0.085	0.831	0.089	0.06	0.316	0.011	C3
Voltage normal	12.8 kHz	0.006	0.945	0	0	0	0	C1
Current transient + harmonics (Fig. 4(c))	12.8 kHz	1.605	0.821	1.876	0.635	0.812	0.048	C16

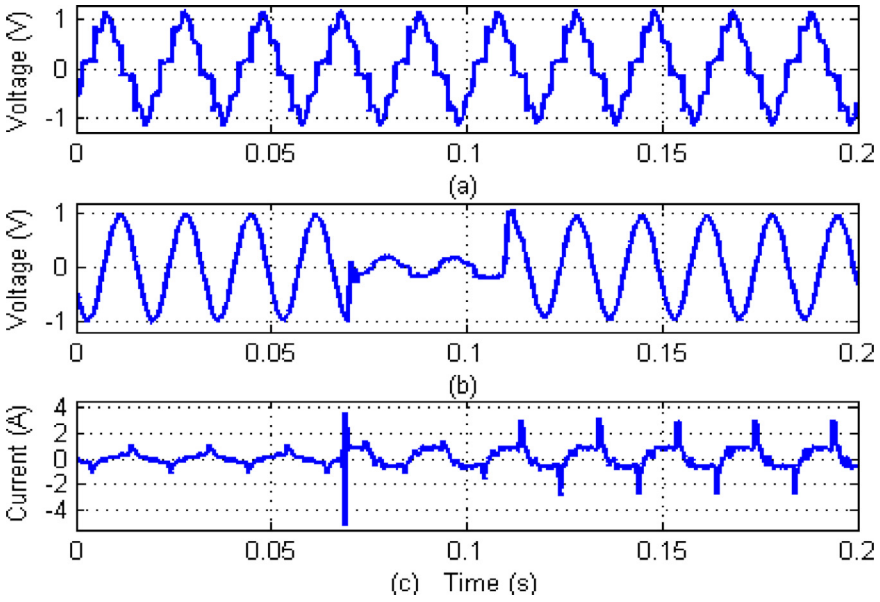

Fig. 4. Measured power quality disturbances.

Table 7
Performance comparison of the different methods.

Method	No. of Features	No. of disturbance classes	Accuracy (%)
Ref [8]	5	11	98.2
Ref [14]	5	14	97.28
Ref [15]	19	9	99.66
Ref [44]	10	5	98.51
Ref [45]	45	22	99.09
Ref [46]	2	10	94.2
Proposed method	6	9	97.22
		16	95.56
		21	88.48

online PQ monitoring device. The proposed method uses a minimal set of features to attain reasonable classification accuracy with less computation.

5. Conclusion

This paper presents an automatic approach based on an adaptive filtering and a multiclass SVM for classification of single and the most frequent combined disturbances. The EWT-based adaptive filtering technique initially estimates the frequencies based on the divide to conquer principle and then designed the filters adaptively. The computational advantage of the FFT and adaptiveness of the filter design makes the technique suitable for decomposing the distortion signal perfectly and fast. The feature plot reveals that the extracted six features contain significant information, which reflects the distortions precisely and are easy to extract. Further, the mapping potentiality of the multiclass SVM has been successfully utilized to recognize multiple disturbances. The multiclass SVM adopting one-against-one (OAO) method with the polynomial kernel is superior to the other kernels and one-against-all (OAA) method. Finally, the experiments carried out with the simulated as well as a few measured power disturbance signals prove the accuracy, shows robustness to noise and practical applicability of the proposed approach with OAA-SVM.

References

[1] R.C. Dugan, M.F. Mc Granaghan, H.W. Beaty, Electrical Power Systems Quality, McGraw-Hill, New York, 2012.
[2] IEEE Recommended Practice for Monitoring Electric Power Quality. (2009) IEEE Std. 1159–2009.
[3] M.H.J. Bollen, Understanding Power Quality Problems: Voltage Sags and Interruptions, IEEE press, New York, 2000.
[4] J.V. Milanovic, J. Meyer, R.F. Ball, W. Howe, R. Preece, et al., International industry practice on power quality monitoring, IEEE Trans. Power Del. 29 (2) (2014) 934–941.
[5] H. Math, J. Bollen, I.Y. Gu, Signal Processing of Power Quality Disturbances (2006).
[6] D. Gra-nados-Lieberman, R.J. Romero-Troncoso, R.A. Osornio-Rios, A. Garcia-Perez, E. Cabal-Yepez, Techniques and methodologies for power quality analysis and disturbances classification in power systems: a review, IET Gener, Transm. Distrib. 5 (4) (2011) 519–529.
[7] M.K. Saini, R. Kapoor, Classification of power quality events – a review, Int. J Electr. Power Energy Syst. 43 (2012) 11–19.
[8] Chun-Yao Lee, Yi-Xing Shen, Optimal feature selection for power-quality disturbances classification, IEEE Trans. Pow. Del. 26 (4) (2011) 2342–2351.
[9] S.A. Deokar, L.M. Waghmare, Integrated dwt-fft approach for detection and classification of power quality disturbances, Int. J. Electr. Power Energy Syst. 61 (2014) 594–605.
[10] K. Manimala, K. Selvi, R. Ahila, Optimization techniques for improving power quality data mining using wavelet packet based support vector machine, Neurocomputing 77 (1) (2012) 36–47.
[11] S. Zhang, P. Li, L. Zhang, H. Li, W. Jiang, Y. Hu, Modified S transform and ELM algorithms and their applications in power quality analysis, Neurocomputing 185 (12) (2016) 231–241.
[12] B.K. Panigrahi, P.K. Dash, J.B.V. Reddy, Hybrid signal processing and machine intelligence techniques for detection, quantification and classification, Eng. Appl. Artif. Intell. 22 (3) (2009) 442–452.

[13] T. Jayasree, D. Devaraj, R. Sukanesh, Power quality disturbance classification using Hilbert transform and RBF networks, Neurocomputing 73 (7–9) (2010) 1451–1456.
[14] K. Thirumala, S.P. Maganuru, T. Jain, A.C. Umarikar, Tunable-Q wavelet transform and dual multiclass SVM for online automatic detection of power quality disturbances, IEEE Trans. Smart Grid 2016 9 (4) (2018) 3018–3028.
[15] Ali A Abdoos, P.K. Mianaei, M.R. Ghadikolaei, Combined VMD-SVM based feature selection method for classification of power quality events, Appl. Soft Comput. 38 (2016) 637–646.
[16] M. Zhang, K. Li, Y. Hu, A real time classification method for power quality disturbances, Electric Power Syst. Res. 81 (1) (2011) 660–666.
[17] M. Biswal, P.K. Dash, Detection and characterization of multiple power quality disturbances with a fast S transform and decision tree based classifier, Digital Signal Process. 23 (4) (2013) 1071–1083.
[18] H.S. Behera, P.K. Dash, B. Biswal, Power quality time series data mining using S-transform and fuzzy expert system, Appl. Soft Comput. 10 (3) (2010) 945–955.
[19] E. Styvaktakis, M.H.J Bollen, I.Y.H. Gu, Expert system for classification and analysis of power system events, IEEE Trans. Power Del. 17 (2) (2002) 423–428.
[20] A.M. Gaouda, S.H. Kanoun, M.M.A. Salama, On-line disturbance classification using nearest neighbor rule, Electric Power Syst. Res. 57 (1) (2001) 1–8.
[21] B.K. Panigrahi, V.R. Pandi, Optimal feature selection for classification of power quality disturbances using wavelet packet-based fuzzy k-nearest neighbour algorithm, IET Gen. Transm. Distrib. 3 (3) (2009) 296–306.
[22] L. Chiung-Chou, Enhanced RBF network for recognizing noise-riding power quality events, IEEE Trans. Power Del. 59 (6) (2010) 1550–1561.
[23] Z. Liu, Q. Zhang, Z. Han, G. Chen, A new classification method for transient power quality combining spectral kurtosis with neural network, Neurocomputing 125 (2014) 95–101.
[24] G.-S. Hu, F.-F. Zhu, Z. Ren, Power quality disturbance identification using wavelet packet energy entropy and weighted support vector machines, Exp. Syst. Appl. 35 (1–2) (2008) 143–149.
[25] W.M. Lin, C.H. Wu, C.H. Lin, F.S. Cheng, Detection and classification of multiple power-quality disturbances with wavelet multiclass SVM, IEEE Trans. Power Del. 23 (4) (2008) 2575–2582.
[26] Z. Liu, Y. Cui, W. Li, A classification method for complex power quality disturbances using EEMD and rank wavelet SVM, IEEE Trans. Smart Grid 6 (4) (2015) 1678–1685.
[27] D.D. Ferreira, J.M. de Seixas, A.S. Cerqueira, A method based on independent component analysis for single and multiple power quality disturbance classification, Electric Power Syst. Res. 119 (2015) 425–431.
[28] M.V. Rodriguez, R.D.J.R. Troncoso, R.A.O. Rios, A.G. Perez, Detection and classification of single and combined power quality disturbances using neural networks, IEEE Trans. Ind. Electron. 61 (5) (2014) 2473–2482.
[29] C.M. Luciano, Mario Oleskovicz A., A.S. Ricardo Fernandes, Adaptive threshold based on wavelet transform applied to the segmentation of single and combined power quality disturbances, Appl. Soft Comput. 38 (2016) 967–977.
[30] IEC standard 61000-4-7. General guide on harmonics and interharmonics measurements, for power supply systems and equipment connected thereto, 2002.
[31] T. Tarasiuk, Comparative study of various methods of DFT calculation in the wake of IEC Standard 61000-4-7, IEEE Trans. Instrum. Meas. 58 (10) (2009) 3666–3677.
[32] B. Zeng, Y. Zhou, Z. Teng, G. Li, A novel approach for harmonic parameters estimation under nonstationary situations, Int. J. Elect. Power Energy Syst. 44 (1) (2013) 930–937.
[33] D. Gallo, R. Langella, A. Testa, Desynchronized processing technique for harmonic and interharmonic analysis, IEEE Trans. Power Del. 19 (3) (2004) 993–1001.
[34] C.M. Orallo, I. Carugati, S. Maestri, et al., Harmonics measurement with a modulated sliding discrete fourier transform algorithm, IEEE Trans. Instrum. Meas. 63 (4) (2014) 781–793.
[35] J. Gilles, Empirical wavelet transform, IEEE Trans. Signal Process 61 (16) (2013) 3999–4010.
[36] J. Gilles, G. Tran, S. Osher, 2d empirical transforms. wavelets, ridgelets, and curvelets revisited, SIAM J. Imag. Sci. 7 (1) (2014) 157–186.
[37] K. Thirumala, A. Umarikar, T. Jain, Estimation of single-phase and three-phase power-quality indices using empirical wavelet transform, IEEE Trans. Power Del. 30 (1) (2015) 445–454.
[38] S.L. Hahn, Hilbert Transforms in Signal Processing, Artech House, Boston, London, 1996.
[39] C. Cortes, V. Vapnik, Support vector networks, Mach. Learn. 20 (1995) 273–297.
[40] C.W. Hsu, C.J. Lin, A comparison of methods for multiclass support vector machines, IEEE Trans. Neural Netw. 13 (2) (2002) 415–425.
[41] C.C. Chang, C.J. Lin, LIBSVM: a library for support vector machines, ACM Trans. Intel. Syst. Technol. 2 (2011) 1–27. Available http://www.csie.ntu.edu.tw/~cjlin/libsvm .
[42] V.K. Tiwari, S.K. Jain, Hardware implementation of polyphase-decomposition-based wavelet filters for power system harmonics estimation, IEEE Trans. Inst. Meas. 65 (7) (2016) 1585–1595.
[43] IEEE 1159.2 Working group, Test waveforms. http://grouper.ieee.org/groups/1159/2/testwave.html [Available Online].
[44] H. Eristi, Y. Demir, Automatic classification of power quality events and disturbances using wavelet transform and support vector machines, IET Gen. Trans. Distrib. 6 (10) (2012) 968–976.
[45] S. Dalai, D. Dey, B. Chatterjee, S. Chakravorti, K. Bhattacharya, Cross-spectrum analysis-based scheme for multiple power quality disturbance sensing device, IEEE Sens. J. 15 (7) (2015) 3989–3997.
[46] M.D. Barras, J.C. Bravo, J.C. Montano, Disturbance ratio for optimal multi-event classification in power distribution networks, IEEE Trans. Ind. Elect. 63 (5) (2016) 3117–3124.

Karthik Thirumala is an Assistant Professor in the Department of Electrical and Electronics Engineering, National Institute of Technology Tiruchirappalli, Tiruchirappalli, India. His research interest includes power quality and power electronic applications to power system.

Sushmita Pal received the B.Tech degree in Electrical Engineering from the Indian Institute of Technology Indore, Indore, India in 2016. Her research interests include power quality analysis and artificial intelligence.

Trapti Jain is an Associate Professor in the Department of Electrical Engineering, Indian Institute of Technology Indore, Indore, India. Her research interests include power systems security, artificial-intelligence applications to power systems, power system dynamics, and power quality.

Amod C. Umarikar is an Associate Professor in the Department of Electrical Engineering, Indian Institute of Technology Indore, Indore, India. His research interests include the application of power electronics in renewable energy systems and power quality.